

Kerr black hole shadows from axion-photon coupling

Songbai Chen^{1,2*}, Jiliang Jing^{1,2} [†]

¹ *Department of Physics, Institute of Interdisciplinary Studies,
Key Laboratory of Low Dimensional Quantum Structures and Quantum Control of Ministry of Education,
Synergetic Innovation Center for Quantum Effects and Applications,
Hunan Normal University, Changsha, Hunan 410081, People's Republic of China*

² *Center for Gravitation and Cosmology, College of Physical Science and Technology,
Yangzhou University, Yangzhou 225009, People's Republic of China*

Abstract

We have investigated the motion for photons in the Kerr black hole spacetime under the axion-photon coupling. The birefringence phenomena arising from the axion-photon coupling can be negligible in the weak coupling approximation because the leading-order contributions to the equations of motion come from the square term of the coupling parameter. We find that the coupling parameter makes the size of shadows slightly increase for arbitrary spin parameter. For the rapid rotating black hole case with a larger coupling, we find that there exist a “pedicel”-like structure appeared in the left of the “D”-type like shadows. Comparing the shadow size of the Kerr black hole with the shadow size of the Sgr A* and M87* black holes, we make constraints on the parameter space for such a theoretical model of the axion-photon coupling.

PACS numbers: 04.70.Dy, 95.30.Sf, 97.60.Lf

* Corresponding author: csb3752@hunnu.edu.cn

[†] jljing@hunnu.edu.cn

I. INTRODUCTION

The images of the supermassive black holes M87* [1–4] and Sgr A* [5, 6] open a new window to test gravity in strong field regimes. Meanwhile, they also provide a powerful way to probe electromagnetic interactions, matter distributions and accretion processes near black holes [7–17]. With the circularity and size of its first image, the rotational nature of the supermassive object M87* was tested [18] and the Kerr black hole hypothesis was further examined [19]. The image features of black holes with extra hairs have been extensively studied [20–25], which could provide a way to check no-hair theorem in the strong gravity region. Moreover, the supermassive black hole images have been applied to probe the Lorentz symmetry violation [26–28], hunt extra dimensions [29, 30], test Loop quantum gravity [31–33] and examine other alternative theories [34, 35]. The black hole images have also been studied in the Euler-Heisenberg and Bronnikov non-linear electrodynamics models coupled to general relativity [36]. The main component in the black hole’s image is the shadow, which is caused by light rays that fall into an outer event horizon. In general, the black hole shadow depends on the parameters of black hole backgrounds, the propagations of light rays and the positions of observers. Recent studies also show that the some interactions between electromagnetic and gravitational fields leads to birefringence of photons in spacetimes, which result in double shadows for a single black hole [37–42]. These interesting features have triggered the further study of black hole shadows under interactions between electromagnetic and other fields. A phenomenological coupling between a photon and a generic vector field is also introduced to study black hole shadows [43], which shows that the black hole shadow in edge-on view has different appearances for different frequencies of the observed lights.

Dark matter is widely believed to be the dominant gravitationally attractive component in the Universe although its nature is still unclear. One of the most interesting candidates for dark matter is axion, which is hypothetical pseudoscalar particle initially introduced by Peccei and Quinn [44] to solve the strong charge-conjugation and parity problem in quantum chromodynamics. Interestingly, axion is also furthermore generically predicted in string theory [45–47]. One of the important properties of axions is that they interact with photons through the coupling, which leads to an interesting conversion from photons into axions and vice versa in the presence of a magnetic field [48, 49]. Such axion-photon conversion is also regarded as basic principle [50, 51] to experimentally detect Solar axions [52–54] and axion dark matter [55]. Moreover, to account for the recent detections of high-energy gamma ray photons from extragalactic sources, some suggestions [56, 57] based on the axion-photon conversion are introduced because the conversion can prevent the

high-energy photons from being annihilated through electron-positron pair production in their propagations. Recent investigations [58–60] show that the resonant axion-photon conversion inside the cluster’s magnetic field could distort the black-body spectrum of the cosmic microwave background.

As a coupling between matter and electromagnetic fields, the axion-photon coupling also results in the photon birefringence [61] as photon crosses over axion matter. The birefringence effects of the polarization photons have been used to analyze the axion dark matter distribution near M87* black hole [62] and in the protoplanetary disk around a young star [63]. The axion-induced birefringence effect gives arise to the unique polarimetric structure [64] and the electric vector position angle oscillation of linearly polarized photons [65]. Such oscillation has been applied to constrain region of the axion mass and axion-photon coupling parameter space together with the observation data from Event Horizon Telescope [65]. Moreover, the conversion of photons into axions leads to a dimming of the photon ring around the black hole shadow [66]. The photon scattering from the background magnetic field with axions is also found to generate a significant circular polarization around the horizon of supermassive black hole [67] and in blazars [68]. The polarization-dependent bending that a ray of light experiences by traveling through an axion cloud is studied in the background of a Kerr black hole [69]. All above literature is focused on analyzing effects of the axion-photon coupling on the brightness and polarization patterns of surrounding emissions region in black hole images. However, it is still an open issue how the axion-photon coupling affect black hole shadows. In this paper, we start from the modified Maxwell equation and make use of the geometric optics approximation to obtain the equation of motion for the photon coupling to an axion field. Then, we probe the effects of axion-photon coupling on the shadow of a rotating black hole.

The paper is organized as follows: In Sec.II, we firstly present equation of motion for photons interacted with axion-like particles in the Kerr black hole spacetime and obtain two kind of solutions of polarized photon motions. In Sec.III, we present numerically Kerr black hole shadows under the axion-photon coupling and probe its effects on the shadows. Finally, we end the paper with a summary.

II. EQUATION OF MOTION FOR THE PHOTONS COUPLING AXION-LIKE PARTICLES IN A KERR BLACK HOLE SPACETIME

We firstly present the equations of motions for photons interacted with axion-like particles in a Kerr black hole spacetime by the geometric optics approximation [70–74]. In the curved spacetime, the action contained

the coupling between photon and axion-like particle can be expressed as [44, 48–51, 61]

$$S = \int d^4x \sqrt{-g} \left[\frac{R}{16\pi G} + \frac{1}{2} \partial_\mu \psi \partial^\mu \psi - \frac{1}{4} \left(F_{\mu\nu} F^{\mu\nu} - \alpha \psi F_{\mu\nu} \tilde{F}^{\mu\nu} \right) \right], \quad (1)$$

where ψ denotes the axion-like field and $\tilde{F}^{\mu\nu} = \epsilon^{\mu\nu\rho\sigma} F_{\rho\sigma}/2$ is the dual of the electromagnetic field strength tensor. $\epsilon^{\mu\nu\rho\sigma}$ is the Levi-Civita tensor and α denotes the axion-photon coupling constant with dimensions of inverse energy. Generally, the axion-like field ψ is dynamical. Here, we assume it as a function of a radial and polar angle coordinate $\psi = \psi(r, \theta)$ for the sake of simplicity. Therefore, the coupling between photon and axion-like particle modifies Maxwell equation as

$$\nabla_\mu F^{\mu\nu} - 2\alpha \psi_\mu \epsilon^{\mu\nu\rho\sigma} F_{\rho\sigma} = 0, \quad (2)$$

where $\psi_\mu \equiv \partial_\mu \psi$. Using the geometric optics approximation [70–74], we can get equation of motions for coupled photons from the modified Maxwell equation (2). In this approximation, the wavelengths of photons are assumed to be much smaller than a typical curvature scale, but be larger than the electron Compton wavelength. Then, the electromagnetic tensor $F_{\mu\nu}$ can be rewritten as a simpler form

$$F_{\mu\nu} = f_{\mu\nu} e^{i\theta}, \quad (3)$$

with a slowly varying amplitude $f_{\mu\nu}$ and a rapidly varying phase θ . Comparing with the wave vector $k_\mu = \partial_\mu \theta$, one can find that the derivative term $f_{\mu\nu;\lambda}$ can be neglected since it is not dominated in this case. Making use of the Bianchi identity

$$D_\lambda F_{\mu\nu} + D_\mu F_{\nu\lambda} + D_\nu F_{\lambda\mu} = 0, \quad (4)$$

it is easy to obtain that the form of the amplitude $f_{\mu\nu}$ must be

$$f_{\mu\nu} = k_\mu a_\nu - k_\nu a_\mu. \quad (5)$$

Here the polarization vector a_μ is orthogonal to the wave vector k_μ , i.e., $k_\mu a^\mu = 0$. Inserting Eqs.(3) and (5) into Eq. (2), we can obtain the modified equation of motions for photons under the axion-photon coupling

$$k_\mu k^\mu a^\nu - i4\alpha \psi_\mu \epsilon^{\mu\nu\rho\sigma} k_\sigma a_\rho = 0, \quad (6)$$

which means that the coupling will change the propagation of photons in background spacetimes.

With the standard Boyer-Lindquist coordinates, the metric of a Kerr black hole can be expressed as

$$ds^2 = -\rho^2 \frac{\Delta}{\Sigma^2} dt^2 + \frac{\rho^2}{\Delta} dr^2 + \rho^2 d\theta^2 + \frac{\Sigma^2}{\rho^2} \sin^2 \theta (d\phi - \omega dt)^2, \quad (7)$$

with

$$\begin{aligned}\omega &= \frac{2aMr}{\Sigma^2}, & \rho^2 &= r^2 + a^2 \cos^2 \theta, \\ \Delta &= r^2 - 2Mr + a^2, & \Sigma^2 &= (r^2 + a^2)^2 - a^2 \sin^2 \theta \Delta.\end{aligned}\quad (8)$$

Here the parameters M and a denote the mass and the spin parameter of the black hole, respectively. For the Kerr black hole spacetime, it is convenient to build a local set of orthonormal frames by introducing vierbein fields e_μ^a obeyed the condition

$$g_{\mu\nu} = \eta_{ab} e_\mu^a e_\nu^b, \quad (9)$$

where η_{ab} denotes the Minkowski metric. The forms of the vierbein fields e_μ^a and their inverse e_a^μ can be respectively expressed as

$$e_\mu^a = \begin{pmatrix} \rho \frac{\sqrt{\Delta}}{\Sigma} & 0 & 0 & -\frac{\omega \Sigma}{\rho} \sin \theta \\ 0 & \frac{\rho}{\sqrt{\Delta}} & 0 & 0 \\ 0 & 0 & \rho & 0 \\ 0 & 0 & 0 & \frac{\Sigma}{\rho} \sin \theta \end{pmatrix}, \quad (10)$$

and

$$e_a^\mu = \begin{pmatrix} \frac{\Sigma}{\rho \sqrt{\Delta}} & 0 & 0 & 0 \\ 0 & \frac{\sqrt{\Delta}}{\rho} & 0 & 0 \\ 0 & 0 & \frac{1}{\rho} & 0 \\ \frac{\omega \Sigma}{\rho \sqrt{\Delta}} & 0 & 0 & \frac{\rho}{\Sigma \sin \theta} \end{pmatrix}. \quad (11)$$

Making use of the relationship $a^\mu k_\mu = 0$, one can find that the equation of motion of the photon coupling with axion can be simplified as a set of equations for three independent polarisation components a^r , a^θ , and a^ϕ ,

$$\begin{pmatrix} K_{11} & K_{12} & K_{13} \\ K_{21} & K_{22} & K_{23} \\ K_{31} & K_{32} & K_{33} \end{pmatrix} \begin{pmatrix} a^r \\ a^\theta \\ a^\phi \end{pmatrix} = 0. \quad (12)$$

The coefficients K_{ij} are very complicated and here we do not list them. The necessary and sufficient condition for Eq.(12) to have non-zero solutions is that the determinant of its coefficient matrix is zero. Solving the equation $|K| = 0$, we obtain two non-zero physical solutions,

$$g_{\mu\nu} \dot{x}^\mu \dot{x}^\nu \pm 4\alpha \sqrt{(\psi_\mu \dot{x}^\mu)^2 + 4\alpha^2 (\psi_\mu \psi^\mu)^2} + 8\alpha^2 \psi_\mu \dot{x}^\mu = 0. \quad (13)$$

This means that the coupling between photon and axion-like scalar field could give arise to birefringence phenomena, even if in the non-rotating case. The light cone condition (14) implies that the coupling photons propagate along non-geodesic paths in the Kerr spacetime. Considered that the coupling parameter α is small

for physically justification, the left side of the equation (13) can be expanded as an Taylor series near $\alpha = 0$. Neglecting its higher terms $\mathcal{O}(\alpha^3)$, we find that the equation (13) can be further approximated as

$$g_{\mu\nu}\dot{x}^\mu\dot{x}^\nu \pm 4\alpha\psi_\mu\dot{x}^\mu + 8\alpha^2\psi_\mu\psi^\mu = 0. \quad (14)$$

Thus, the motion of the coupling photon can be actually determined by a Lagrange function

$$\mathcal{L} = \frac{1}{2}g_{\mu\nu}\dot{x}^\mu\dot{x}^\nu \pm 2\alpha\psi_\mu\dot{x}^\mu + 4\alpha^2\psi_\mu\psi^\mu. \quad (15)$$

From the previous discussion, under the geometric optics approximation [70–74], we have $F_{\mu\nu} = f_{\mu\nu}e^{i\theta} = (k_\mu a_\nu - k_\nu a_\mu)e^{i\theta}$ and then the coupling term $\alpha F_{\mu\nu}\tilde{F}^{\mu\nu}$ in the Klein-Gordon equation becomes

$$\alpha F_{\mu\nu}\tilde{F}^{\mu\nu} = \frac{\alpha}{2}\epsilon^{\mu\nu\rho\sigma}F_{\mu\nu}F_{\rho\sigma} = 2\alpha\epsilon^{\mu\nu\rho\sigma}k_\mu a_\nu k_\rho a_\sigma e^{2i\theta} = 0, \quad (16)$$

which means that under geometric optics approximation, the coupling photons do not change the distribution of the scalar field in the spacetime. Here, we assume that the scalar field possesses the same symmetry as the Kerr spacetime and has a form $\psi = \psi(r, \theta)$, then the corresponding Klein-Gordon equation becomes

$$\frac{1}{\sqrt{-g}}\frac{d}{dr}\left(\sqrt{-g}g^{rr}\frac{d\psi(r, \theta)}{dr}\right) + \frac{1}{\sqrt{-g}}\frac{d}{d\theta}\left(\sqrt{-g}g^{\theta\theta}\frac{d\psi(r, \theta)}{d\theta}\right) = 0. \quad (17)$$

Assuming the scalar field has a form $\psi(r, \theta) = \mathcal{R}(r)\Theta(\theta)$ in the Kerr spacetime, we have

$$\frac{1}{\mathcal{R}(r)}\frac{d}{dr}\left(\Delta\frac{d\mathcal{R}(r)}{dr}\right) = -\frac{1}{\Theta(\theta)\sin\theta}\frac{d}{d\theta}\left(\sin\theta\frac{d\Theta(\theta)}{d\theta}\right) = l(l+1). \quad (18)$$

It is easy to find that the general solution of Eq. (18) is

$$\mathcal{R}(r) = C_1 P_l\left(\frac{r-M}{\sqrt{M^2-a^2}}\right) + C_2 Q_l\left(\frac{r-M}{\sqrt{M^2-a^2}}\right), \quad \Theta(\theta) = C_3 P_l(\cos\theta) + C_4 Q_l(\cos\theta). \quad (19)$$

Where $P_l(x)$ and $Q_l(x)$ are the Legendre functions of the first and second kinds, respectively. C_i ($i = 1, 2, 3, 4$) are the corresponding integration constants. For the sake of simplicity, we set $l = 1$, $C_1 = \frac{\pi^i}{2}C_2$, $C_2 = C_3 = C$ and $C_4 = 0$, where C is assumed to be positive without loss of generality. This special solution of scalar field is not divergent at the spatial infinity and has a form

$$\psi(r, \theta) = C \left[\frac{r-M}{2\sqrt{M^2-a^2}} \ln \frac{r-r_-}{r-r_+} - 1 \right] \cos\theta, \quad (20)$$

where $r_\pm = M \pm \sqrt{M^2 - a^2}$. The radial part $\psi_R \equiv \frac{r-M}{2\sqrt{M^2-a^2}} \ln \frac{r-r_-}{r-r_+} - 1$ decreases with the coordinate r . The boundaries of black hole shadows depend on the marginally unstable circular orbits of photons. From Fig.1, we find that the absolute value $|\psi_R| < 1$ in the region outside the marginally unstable circular orbit of photons even if in the rapidly rotation case. Thus, in the propagation of lights reaching the spatial infinity, the scalar

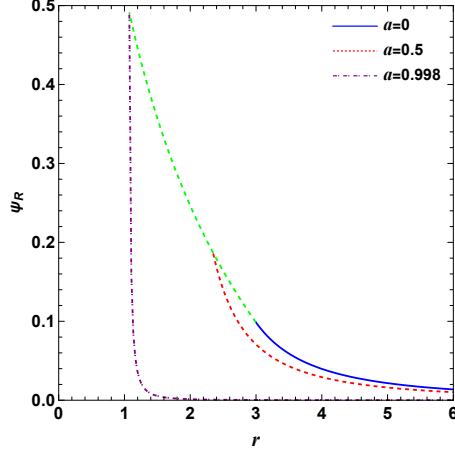


FIG. 1: Change of the radial part ψ_R of the scalar field in Eq.(20) with the coordinate r in the region outside the marginally unstable circular orbit of photons for different spin parameter a . The green dashed line corresponds to the curve $\psi_R - r_{ph}$, where r_{ph} is the marginally unstable circular radius of photon.

field meets the condition $|\psi| < C$. With the form of scalar field in Eq. (20), we can obtain its derivative with respect to coordinates x^μ

$$\psi_\mu = C \left[0, \left(\frac{1}{2\sqrt{M^2 - a^2}} \ln \frac{r - r_-}{r - r_+} - \frac{r - M}{\Delta} \right) \cos \theta, - \left(\frac{r - M}{2\sqrt{M^2 - a^2}} \ln \frac{r - r_-}{r - r_+} - 1 \right) \sin \theta, 0 \right]. \quad (21)$$

Inserting Eq.(21) into Eq.(15), we find that the Lagrange function \mathcal{L} is independent of the coordinates t and ϕ , the photon's energy E_0 and its z -component of the angular momentum L_{z0} are two conserved quantities as in the case without the coupling. With these two conserved quantities and the Lagrange-Euler equation, we can obtain the equation of motion of the coupling photon

$$\dot{t} = \frac{g_{\phi\phi}E_0 + g_{t\phi}L_{z0}}{g_{t\phi}^2 - g_{tt}g_{\phi\phi}}, \quad \dot{\phi} = \frac{g_{t\phi}E_0 + g_{tt}L_{z0}}{g_{tt}g_{\phi\phi} - g_{t\phi}^2}, \quad (22)$$

$$\ddot{r} = \frac{1}{2g_{rr}} \left[g_{tt,r}\dot{t}^2 - g_{rr,r}\dot{r}^2 - 2g_{rr,\theta}\dot{r}\dot{\theta} + g_{\theta\theta,r}\dot{\theta}^2 + g_{\phi\phi,r}\dot{\phi}^2 + 2g_{t\phi,r}\dot{t}\dot{\phi} + 8\alpha^2 \frac{\partial}{\partial r} \left(\psi_\mu \psi^\mu \right) \right], \quad (23)$$

$$\ddot{\theta} = \frac{1}{2g_{\theta\theta}} \left[g_{tt,\theta}\dot{t}^2 + g_{rr,\theta}\dot{r}^2 - 2g_{\theta\theta,r}\dot{r}\dot{\theta} - g_{\theta\theta,\theta}\dot{\theta}^2 + g_{\phi\phi,\theta}\dot{\phi}^2 + 2g_{t\phi,\theta}\dot{t}\dot{\phi} + 8\alpha^2 \frac{\partial}{\partial \theta} \left(\psi_\mu \psi^\mu \right) \right]. \quad (24)$$

Here we note that the term $\pm 2\alpha\psi_\mu \dot{x}^\mu$ has no contribution to the equations of motion of the coupling photons since the force arising from this term is $\pm 2\alpha g^{\mu\nu}(\psi_{\rho,\mu} - \psi_{\mu,\rho})\dot{x}^\rho$, which is zero because the scalar field ψ is a continuous function and its second-order partial derivative is independent of the sequence of derivation. The leading-order contributions to the equations of motion (Eqs.(23) and (24)) come from the corrected terms contained the factor α^2 , which implies that the birefringence phenomena may be negligible in the small α approximation. In the next section, we will study the effects of the axion-photon coupling on Kerr black hole shadows.

III. SHADOW OF KERR BLACK HOLE UNDER THE AXION-PHOTON COUPLING

To obtain the shadow of Kerr black hole under the axion-photon coupling, we must adopt the “backward ray-tracing” method as in [20–23, 76–82] because the motion equations (22)-(24) can not be variable-separable. With this method, the position of each pixel in the final image can be got by solving numerically the nonlinear differential equations (22)-(24) by assuming that light rays evolve from the observer backward in time. The black hole shadow in observer’s sky is determined only by the pixels related to the light rays falling down into black hole. For the Kerr spacetime (7), the transformation between the local basis of observer $\{e_{\hat{t}}, e_{\hat{r}}, e_{\hat{\theta}}, e_{\hat{\phi}}\}$ and the coordinate basis of the background spacetime $\{\partial_t, \partial_r, \partial_\theta, \partial_\phi\}$ can be expressed as

$$e_{\hat{\mu}} = e_{\hat{\mu}}^\nu \partial_\nu, \quad (25)$$

and the transformation matrix $e_{\hat{\mu}}^\nu$ satisfies $g_{\mu\nu} e_{\hat{\alpha}}^\mu e_{\hat{\beta}}^\nu = \eta_{\hat{\alpha}\hat{\beta}}$, where $\eta_{\hat{\alpha}\hat{\beta}}$ is the usual Minkowski metric. For the Kerr spacetime (7), one can conveniently choose the transformation matrix $e_{\hat{\mu}}^\nu$ as

$$e_{\hat{\mu}}^\nu = \begin{pmatrix} \zeta & 0 & 0 & \gamma \\ 0 & A^r & 0 & 0 \\ 0 & 0 & A^\theta & 0 \\ 0 & 0 & 0 & A^\phi \end{pmatrix}, \quad (26)$$

where $\zeta, \gamma, A^r, A^\theta$, and A^ϕ are real coefficients. The decomposition (26) is actually connected with a reference frame with zero axial angular momentum in relation to spatial infinity [76? ? ? ? –82]. According to the Minkowski normalization

$$e_{\hat{\mu}} e^{\hat{\nu}} = \delta_{\hat{\mu}}^{\hat{\nu}}, \quad (27)$$

we obtain the coefficients in the matrix $e_{\hat{\mu}}^\nu$ as

$$\begin{aligned} A^r &= \frac{1}{\sqrt{g_{rr}}}, & A^\theta &= \frac{1}{\sqrt{g_{\theta\theta}}}, & A^\phi &= \frac{1}{\sqrt{g_{\phi\phi}}}, \\ \zeta &= \sqrt{\frac{g_{\phi\phi}}{g_{t\phi}^2 - g_{tt}g_{\phi\phi}}}, & \gamma &= -\frac{g_{t\phi}}{g_{\phi\phi}} \sqrt{\frac{g_{\phi\phi}}{g_{t\phi}^2 - g_{tt}g_{\phi\phi}}}, \end{aligned} \quad (28)$$

With Eq.(25), we further obtain the locally measured four-momentum $p^{\hat{\mu}}$ of photons in the Kerr spacetime (7) as

$$p^{\hat{t}} = \zeta E_0 - \gamma L_{z0}, \quad p^{\hat{r}} = \frac{1}{\sqrt{g_{\phi\phi}}} p_\phi, \quad p^{\hat{\theta}} = \frac{1}{\sqrt{g_{\theta\theta}}} p_\theta, \quad p^{\hat{\phi}} = \frac{1}{\sqrt{g_{rr}}} p_r. \quad (29)$$

Thus, the corresponding celestial coordinates for pixels corresponding to light rays can be expressed as

$$x = -r_{obs} \frac{p^{\hat{\phi}}}{p^{\hat{r}}} = -r_{obs} \frac{\sqrt{g_{rr}}(g_{t\phi}\dot{t} + g_{\phi\phi}\dot{\phi})}{\sqrt{g_{\phi\phi}}(g_{rr}\dot{r} + 2\alpha\psi_r)}, \quad y = r_{obs} \frac{p^{\hat{\theta}}}{p^{\hat{r}}} = r_{obs} \frac{\sqrt{g_{rr}}(g_{\theta\theta}\dot{\theta} + 2\alpha\psi_\theta)}{\sqrt{g_{\theta\theta}}(g_{rr}\dot{r} + 2\alpha\psi_r)}. \quad (30)$$

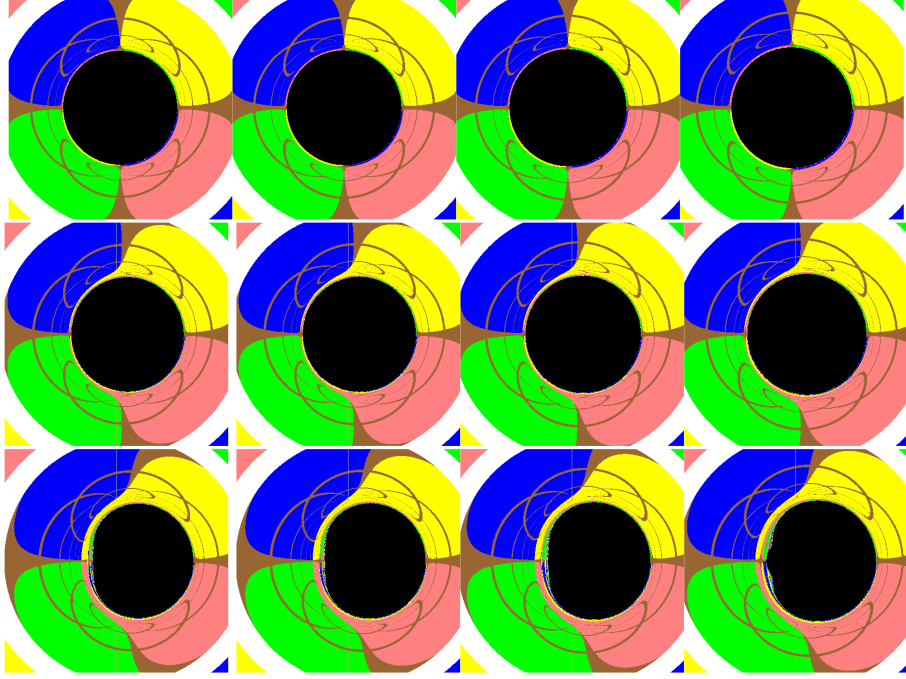


FIG. 2: Shadows of a Kerr black hole casted by the extraordinary rays with different coupling parameter $\tilde{\alpha}$ and spin parameter a for the observer in the equatorial plane ($\theta_{obs} = \pi/2$). The top, middle and bottom rows respectively denote the cases with $a = 0, 0.5$, and 0.998 . In each row, the figures from left to right correspond to $\tilde{\alpha} = 0, 0.1, 0.2$ and 0.3 , respectively. Here we set the mass parameter $M = 1$ and $r_{obs} = 50M$.

where r_{obs} and θ_{obs} are respectively the radial coordinate and polar angle of observer.

Figs.2 and 3 present Kerr black hole shadows under the axion-photon coupling for different spin parameters. To demonstrate the deformation near the black hole arising from strong gravitational lensing, we divide the total celestial sphere into four quadrants painted in different colors (green, blue, red, and yellow) [76? ? ? ? –82] and draw the grids of longitude and latitude lines marked with adjacent brown lines separated by 10° . Actually, the points with different colors in each panel are images of the source points lied in the four different quadrants, which entirely demonstrate the deformation near the black hole originating from strong gravitational lensing. The black parts denote black hole shadows and the white rings provide a direct demonstration of Einstein rings.

Fig.2 presents the Kerr black hole shadows observed in the equatorial plane. It shows that the coupling parameter $\tilde{\alpha} = \alpha C$ results in a larger size of shadows for arbitrary spin parameter a . Moreover, for the rapid rotating black hole, its shadow has a usual “D” type shape as the coupling parameter $\tilde{\alpha}$ is smaller. With the increasing of $\tilde{\alpha}$, we find that there exist a “pedicel”-like structure gradually appeared in the left of the shadow, which is similar to those in shadows of a disformal Kerr black hole in quadratic degenerate higher-order scalar-tensor (DHOST) theory [83]. As the observer stands along the direction of the rotation axis of

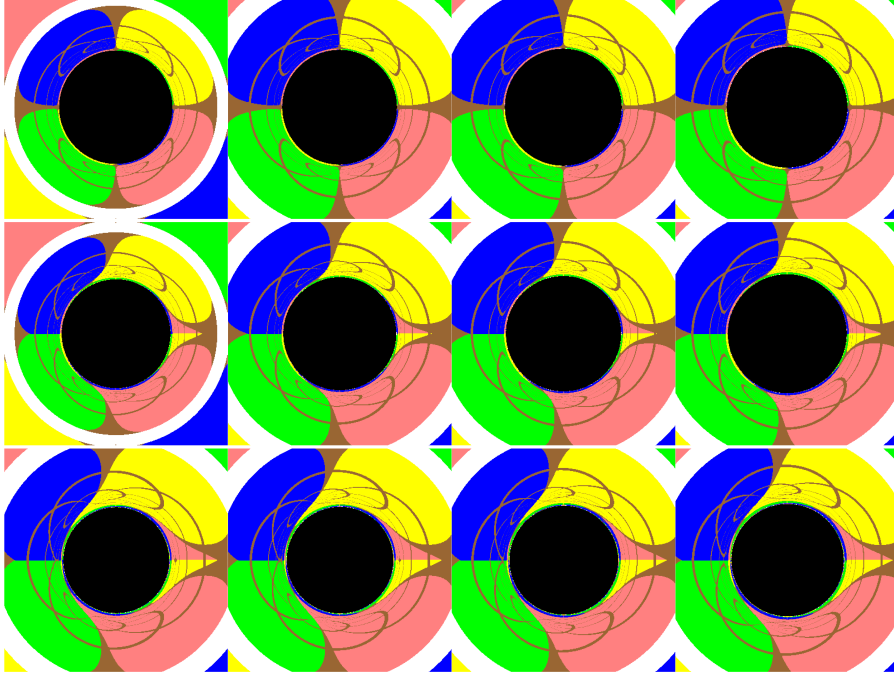


FIG. 3: Shadows of a Kerr black hole casted by the extraordinary rays with different coupling parameter $\tilde{\alpha}$ and spin parameter a for the observer along the rotation axis of black hole ($\theta_{obs} = 0^\circ$). The top, middle and bottom rows respectively denote the cases with $a = 0, 0.5$, and 0.998 . In each row, the figures from left to right correspond to $\tilde{\alpha} = 0, 0.1, 0.2$ and 0.3 , respectively. Here we set the mass parameter $M = 1$ and $r_{obs} = 50M$.

black hole ($\theta_{obs} = 0^\circ$), the black hole shadows in Fig.3 have a shape of a circular disk. With the increase of $\tilde{\alpha}$, the size of shadows slightly increases. This is also consistent with the effects of $\tilde{\alpha}$ on the shadow observed in the equatorial plane.

Let us now to make constraints on the parameter space of the model with axion-photon interaction around black holes using the M87* and Sgr A* images released by the Event Horizon Telescope (EHT) Collaboration. In left panel in Fig. 4, the permissible parameter region (colored) $a - \tilde{\alpha}$ for the model is obtained by using the M87* shadow images with the black hole mass $M = 6.5 \times 10^9 M_\odot$, the observer distance $D_O = 16.8 Mpc$ and the inclination angle $\theta_0 = 17^\circ$. The boundaries of the permissible parameter region are estimated by the angular diameter $39\mu as \leq \theta_d \leq 45\mu as$ [1]. Since the size of shadows increases with the coupling parameter $\tilde{\alpha}$ and decreases with the black hole spin parameter a , the constraints from the M87* show that the smaller coupling parameter is allowable and the larger one is excluded in the case where the black hole is slowly spinning, and the situation is exactly the opposite in the rapidly spinning black hole case. The middle and right panels show the constraints on the parameter space $a - \tilde{\alpha}$ of the model from the Sgr A* shadows with the angular diameter $41.7\mu as \leq \theta_d \leq 55.7\mu as$ [5]. Here we use the mass $M = 4.0 \times 10^6 M_\odot$ and the observer distance $D_O = 8.0 kpc$ for the black hole Sgr A*. Unlike the case M87*, there is no clear consensus on the

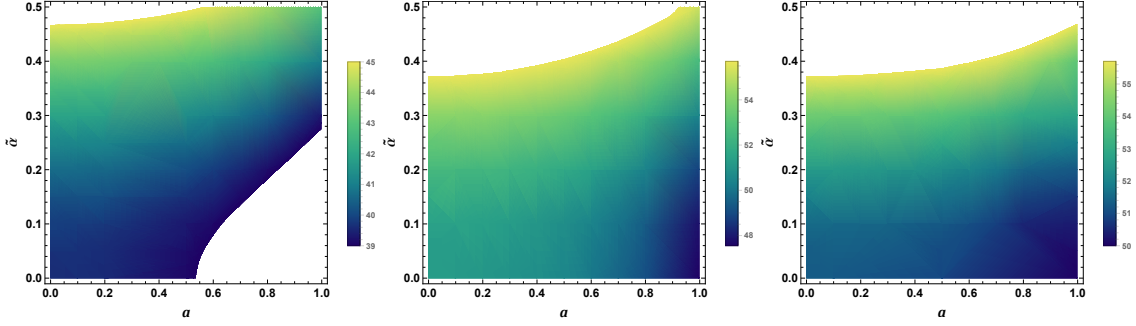


FIG. 4: The permissible parameter region (colored) $a - \tilde{\alpha}$ for the model with axion-photon interaction around black holes using the M87* and Sgr A* shadow images. The left panel is obtained by using the M87* image, where the boundary is estimated by $39\mu\text{as} \leq \theta_d \leq 45\mu\text{as}$. The middle panel and the right one are drawn by using the Sgr A* image with the observed inclination angle $\theta_0 = 0^\circ$ and $\theta_0 = 50^\circ$, respectively. The boundaries in the last two panels are estimated by $41.7\mu\text{as} \leq \theta_d \leq 55.7\mu\text{as}$.

inclination angle θ_0 for the Sgr A* and the current images of the Sgr A* from EHT rule out that the black hole is viewed at high inclination ($\theta_0 \geq 50^\circ$) [5]. Therefore, in Fig.4, we set the observed inclination angle $\theta_0 = 0^\circ$ in the middle panel and $\theta_0 = 50^\circ$ in the right one to get the largest allowable parameter region. The results show that the allowable range of $\tilde{\alpha}$ increases with the black hole spin. In addition, in the rapidly spinning case, the larger inclination angle gives a tighter constraint on the parameter $\tilde{\alpha}$. From Fig.4, it is easy to find that the tightest upper limit of the coupling constant is $\tilde{\alpha} \lesssim 0.5$. The CERN Axion Solar Telescope (CAST) provides a limit on the axion-photon coupling strength $\alpha < 0.66 \times 10^{-10} \text{GeV}^{-1}$ from globular cluster stars [52]. A upper limit on the axion-photon coupling $\alpha < 5.3 \times 10^{-12} \text{GeV}^{-1}$ is recently obtained from the supernova SN1987A [84]. Analyzing the observational data from the Perseus Galaxy Cluster collected with the MAGIC telescopes for NGC 1275, one can find that the limit for axion-like particles is $\alpha < 3 \times 10^{-12} \text{GeV}^{-1}$ [85]. These constraints from observations are performed for the axion-photon coupling constant with dimensions of inverse energy. In this work, the coupling constant $\tilde{\alpha} = \alpha C$ is actually a dimensionless axion photon coupling constant like $c = 2\pi\alpha f_a$, where f_a is the Peccei-Quinn symmetry breaking scale. With data from EHT polarimetric measurements of M87*, one obtains the constraint on the dimensionless coupling constant $c < 0.1$ [62, 65]. Thus, our constraint is a little weaker than that obtained in [62, 65]. These results could help to understand deeply the axion field and their corresponding interactions with electromagnetic field.

IV. SUMMARY

We have investigated the motion for photons in the Kerr black hole spacetime under the axion-photon coupling. Although the axion-photon coupling yields birefringence, the birefringence phenomena can be negligible in the small α approximation because the leading-order contributions to the equations of motion

come from the corrected terms contained the factor α^2 . We also probe the effects of the coupling on the black hole shadows. It shows that the coupling parameter α makes the size of shadows slightly increase for arbitrary spin parameter a . Moreover, for the rapid rotating black hole, its shadow observed in the equatorial plane has a usual “D” type shape as the coupling parameter $\tilde{\alpha}$ is smaller. With the increasing of $\tilde{\alpha}$, we find that there exist a “pedicel”-like structure gradually appeared in the left of the shadow. Finally, we compare the shadow size of the Kerr black hole with those of the Sgr A* and M87* black holes with different coupling values of $\tilde{\alpha}$ and find that there is room for such a theoretical model of the axion-photon coupling. Moreover, in the limit of geometric optics, it is found [86] that the birefringence due to axionic fields is found to be achromatic, but the redshift of light and distance estimates based on propagating light rays, and the shear and magnification due to gravitational lensing are not affected by the interaction of light with an axionic field. These results could help to deeply understand the axion field and their corresponding interactions with electromagnetic field.

V. ACKNOWLEDGMENTS

We thank the referee for the important and insightful comments which are very helpful in the improvement of this work. This work was supported by the National Natural Science Foundation of China under Grant No.12275078, 11875026, 12035005, and 2020YFC2201400, and the innovative research group of Hunan Province under Grant No. 2024JJ1006.

-
- [1] The Event Horizon Telescope Collaboration, *First M87 Event Horizon Telescope Results. I. The Shadow of the Supermassive Black Hole*, *Astrophys. J. Lett.* **875**, L1 (2019).
 - [2] The Event Horizon Telescope Collaboration, *First M87 Event Horizon Telescope Results. VI. The Shadow and Mass of the Central Black Hole*, *Astrophys. J. Lett.* **875**, L6 (2019).
 - [3] Event Horizon Telescope Collaboration, K. Akiyama, J. C. Algaba et al., *First M87 Event Horizon Telescope Results. VII. Polarization of the Ring*, *Astrophys. J. Lett.* **910**, L12 (2021). arXiv:2105.01169
 - [4] Event Horizon Telescope Collaboration, K. Akiyama, J. C. Algaba et al., *First M87 Event Horizon Telescope Results. VIII. Magnetic Field Structure near The Event Horizon*, *Astrophys. J. Lett.* **910**, L13 (2021). arXiv:2105.01173
 - [5] Event Horizon Telescope Collaboration, K. Akiyama, et al., *First Sagittarius A* Event Horizon Telescope Results. I. The Shadow of the Supermassive Black Hole in the Center of the Milky Way*, *Astrophys. J. Lett.* **930**, L12 (2022).
 - [6] Event Horizon Telescope Collaboration, K. Akiyama, et al., *First Sagittarius A* Event Horizon Telescope Results. VI. Testing the Black Hole Metric*, *Astrophys. J. Lett.* **930**, L17 (2022).
 - [7] J. M. Bardeen, *Timelike and null geodesics in the Kerr metric*, in *Black Holes (Les Astres Occlus)*, edited by C. DeWitt and B. DeWitt (Gordon and Breach, New York, 1973), p. 215-239.

- [8] S. Chandrasekhar, *The Mathematical Theory of Black Holes* (Oxford University Press, New York, 1992).
- [9] P. V. P. Cunha, Carlos A. R. Herdeiro, *Shadows and strong gravitational lensing: a brief review*, Gen. Rel. Grav. **50**, 42 (2018).
- [10] V. Perlick, O. Yu, Tsupko, *Calculating black hole shadows: Review of analytical studies*, Phys. Rep. **947**, 1 (2022).
- [11] S. Chen, J. Jing, W. Qian, and B. Wang, *Black hole images: A review*, Sci. China Phys. Mech. Astron. **66**, 260401 (2023).
- [12] M. Wang, S. Chen, J. Jing, *Chaotic shadows of black holes: a short review*, Commun. Theor. Phys. **74**, 097401 (2022).
- [13] X. Liu, S. Chen, and J. Jing, *Polarization distribution in the image of a synchrotron emitting ring around a regular black hole*, Sci. China Phys. Mech. Astron. **65**, 120411(2022).
- [14] S. Wei, Y. Liu, *Testing the nature of Gauss-Bonnet gravity by four-dimensional rotating black hole shadow*, Eur. Phys. J. Plus **136**, 436 (2021), arXiv:2003.07769.
- [15] S. Vagnozzi, et al., *Horizon-scale tests of gravity theories and fundamental physics from the Event Horizon Telescope image of Sagittarius A**, Class. Quant. Grav. **40**, 65007 (2023).
- [16] M. Wang, S. Chen, J. Jing, *Determination of the spin parameter and the inclination angle by the relativistic images in black hole image*, Sci. China Phys. Mech. Astron. **66**, 110411(2023), arXiv:2208.10219.
- [17] J. C. S. Neves, *Geometrization 3.0: the black hole shadow*, arXiv:2212.06054.
- [18] C. Bambi, K. Freese, S. Vagnozzi, L. Visinelli, *Testing the rotational nature of the supermassive object M87* from the circularity and size of its first image*, Phys. Rev. D **100**, 044057 (2019), arXiv:1904.12983.
- [19] K. Glampedakis, G. Pappas, *Can supermassive black hole shadows test the Kerr metric?*, Phys. Rev. D **104**, L081503 (2021).
- [20] P. V. P. Cunha, C. A. R. Herdeiro, E. Radu and H. F. Runarsson, *Shadows of Kerr black holes with scalar hair*, Phys. Rev. Lett. **115**, 211102 (2015).
- [21] P. V. P. Cunha, C. A. R. Herdeiro, E. Radu and H. F. Runarsson, *Shadows of Kerr black holes with and without scalar hair*, Int. J. Mod. Phys. D **25**, 1641021(2016).
- [22] F. H. Vincent, E. Gourgoulhon, C. Herdeiro and E. Radu, *Astrophysical imaging of Kerr black holes with scalar hair*, Phys. Rev. D **94**, 084045 (2016).
- [23] P. V. P. Cunha et al., *Chaotic lensing around boson stars and Kerr black holes with scalar hair*, Phys. Rev. D **94**, 104023 (2016) .
- [24] M. Khodadi, A. Allahyari, S. Vagnozzi, D. F. Motac, *Black holes with scalar hair in light of the Event Horizon Telescope*, J. Cosmol. Astropart. Phys. **09**, 026 (2020), arXiv:2005.05992.
- [25] M. Khodadi, G. Lambiase, D. F. Mota, *No-Hair Theorem in the Wake of Event Horizon Telescope*, J. Cosmol. Astropart. Phys. **09**, 028 (2021).
- [26] M. Khodadi, E. N. Saridakis, *Einstein-Æther gravity in the light of event horizon telescope observations of M87**, Phys. Dark Univ. **32**, 100835 (2021).
- [27] M. Khodadi, G. Lambiase, *Probing the Lorentz Symmetry Violation Using the First Image of Sagittarius A*: Constraints on Standard-Model Extension Coefficients*, Phys. Rev. D **106**, 104050 (2022).
- [28] R. Karmakar, D. J. Gogoi, U. D. Goswami, *Thermodynamics and Shadows of GUP-corrected Black Holes with Topological Defects in Bumblebee Gravity*, Phys. Dark Univ. **41**, 101249 (2023).
- [29] I. Banerjee, S. Chakraborty, S. SenGupta, *Hunting extra dimensions in the shadow of Sgr A**, Phys. Rev. D **106**, 084051 (2022).
- [30] S. Vagnozzi, L. Visinelli, *Hunting for extra dimensions in the shadow of M87**, Phys. Rev. D **100**, 024020 (2019).
- [31] M. Afrin, S. Vagnozzi, S. G. Ghosh, *Tests of Loop Quantum Gravity from the Event Horizon Telescope Results of Sgr A**, Astrophys. J. **944**, 149 (2023).
- [32] H. Jiang, C. Liu, I. K. Dihingiaa, Y. Mizunoa, H. Xu, T. Zhu, Q. Wu, *Shadows of Loop Quantum Black Holes: Semi-analytical Simulations of Loop Quantum Gravity Effects on Sagittarius A* and M87**, J. Cosmol. Astropart. Phys. **01**, 059 (2024).
- [33] C. Liu, T. Zhu, Q. Wu, K. Jusufi, M. Jamil, M. Azreg-Aïnou, A. Wang, *Shadow and Quasinormal Modes of a*

- Rotating Loop Quantum Black Hole*, Phys. Rev. D **101**, 084001 (2020).
- [34] N. Parbin, D. J. Gogoi, U. D. Goswami, *Weak gravitational lensing and shadow cast by rotating black holes in axionic Chern-Simons theory*, Phys. Dark Univ. **41**, 101265 (2023).
 - [35] İ.Çimdiker, A. Övgün, D. Demir, *Thin accretion disk images of the black hole in symmergent gravity*, Class. Quant. Grav. **40**, 184001 (2023).
 - [36] A. Allahyari, M. Khodadi, S. Vagnozzi, D. F. Mota, *Magnetically charged black holes from non-linear electrodynamics and the Event Horizon Telescope*, J. Cosmol. Astropart. Phys. **2002**, 003 (2020), arXiv:1912.08231.
 - [37] Z. Hu, Z. Zhong, Pe. Li, M. Guo, B. Chen, *QED Effect on Black Hole Shadow*, Phys. Rev. D **103**, 044057 (2021).
 - [38] Z. Zhong, Z. Hu, H. Yan, M. Guo, B. Chen, *QED Effects on Kerr Black Hole Shadows immersed in uniform magnetic fields*, Phys. Rev. D **104**, 104028 (2021).
 - [39] X. Zeng, K. He, G. Li, E. Liang, S. Guo, *QED and accretion flow models effect on optical appearance of Euler-Heisenberg black holes*, Eur. Phys. J. C **82**, 764 (2022).
 - [40] Y. Huang, S. Chen, J. Jing, *Double shadow of a regular phantom black hole as photons couple to the Weyl tensor*, Eur. Phys. J. C **76**, 594 (2016).
 - [41] Z. Zhang, S. Chen, X. Qin, J. Jing, *Polarized image of a Schwarzschild black hole with a thin accretion disk as photon couples to Weyl tensor*, Eur. Phys. J. C **81**, 991 (2021).
 - [42] S. Chen, J. Jing, *Kerr black hole shadow casted by the extraordinary light rays with Weyl corrections*, arXiv:2308.16479.
 - [43] C. Li, S. Yan, L. Xue, X. Ren, Y. Cai, D. A. Easson, Y. Yuan, and H. Zhao, *Testing the equivalence principle via the shadow of black holes*, Phys. Rev. Research **2**, 023164 (2020), arXiv:1912.12629 [astro-ph].
 - [44] R. D. Peccei and H. R. Quinn, *CP Conservation in the Presence of Instantons*, Phys. Rev. Lett. **38**, 1440 (1977).
 - [45] A. Arvanitaki, S. Dimopoulos, S. Dubovsky, N. Kaloper, and J. March-Russell, *String Axiverse*, Phys. Rev. D, **81**, 123530 (2010).
 - [46] P. Svrcek, E. Witten, *Axions In String Theory*, J. High Energy Phys. **06**, 051 (2006).
 - [47] D. J. E. Marsh, *Axion Cosmology*, Phys. Rept. **643**, 1 (2016).
 - [48] L. Maiani, R. Petronzio, and E. Zavattini, *Effects of Nearly Massless, Spin Zero Particles on Light Propagation in a Magnetic Field*, Phys. Lett. B **175**, 359 (1986).
 - [49] G. Raffelt and L. Stodolsky, *Mixing of the Photon with Low Mass Particles*, Phys. Rev. D **37**, 1237 (1988).
 - [50] P. Sikivie, *Experimental Tests of the Invisible Axion*, Phys. Rev. Lett. **51**, 1415 (1983), [Erratum: Phys. Rev. Lett. **52**, 695 (1984)].
 - [51] I. G. Irastorza and J. Redondo, *New experimental approaches in the search for axion-like particles*, Prog. Part. Nucl. Phys. **102**, 89 (2018).
 - [52] V. Anastassopoulos et al. (CAST), *New CAST Limit on the Axion-Photon Interaction*, Nature Phys. **13**, 584 (2017).
 - [53] E. Armengaud et al., *Conceptual Design of the International Axion Observatory (IAXO)*, JINST **9**, T05002.
 - [54] A. Banerjee, D. Budker, J. Eby, V. V. Flambaum, H. Kim, O. Matsedonskyi, G. Perez, *Searching for Earth/Solar Axion Halos*, J. High Energy Phys. **09**, 004(2020).
 - [55] S. J. Asztalos et al., *A SQUID-based microwave cavity search for dark-matter axions*, Phys. Rev. Lett. **104**, 041301 (2010).
 - [56] A. Mirizzi and D. Montanino, *Stochastic conversions of TeV photons into axion-like particles in extragalactic magnetic fields*, J. Cosmol. Astropart. Phys. **12**, 004 (2009).
 - [57] M. Meyer, D. Horns, and M. Raue, *First lower limits on the photon-axion-like particle coupling from very high energy gamma-ray observations*, Phys. Rev. D **87**, 035027 (2013).
 - [58] T. Yanagida and M. Yoshimura, *Resonant Axion-Photon Conversion in the Early Universe*, Phys. Lett. B **202**, 301 (1988).
 - [59] A. Mirizzi, J. Redondo, and G. Sigl, *Constraining resonant photon-axion conversions in the Early Universe*, JCAP **08**, 001 (2009).
 - [60] H. Tashiro, J. Silk, and D. J. E. Marsh, *Constraints on primordial magnetic fields from CMB distortions in the*

- axiverse*, Phys. Rev. D **88**, 125024 (2013).
- [61] D. Harari and P. Sikivie, *Effects of a Nambu-Goldstone boson on the polarization of radio galaxies and the cosmic microwave background*, Phys. Lett. B **289**, 67 (1992).
 - [62] Y. Chen, J. Shu, X. Xue, Q. Yuan, Y. Zhao, *Probing Axions with Event Horizon Telescope Polarimetric Measurements*, Phys. Rev. Lett. **124**, 061102 (2020).
 - [63] T. Fujita, R. Tazaki and K. Toma, *Hunting Axion Dark Matter with Protoplanetary Disk Polarimetry*, Phys. Rev. Lett. **122**, 191101 (2019).
 - [64] A. Gußmann, *Polarimetric signatures of the photon ring of a black hole that is pierced by a cosmic axion string*, J. High Energy Phys. **08**, 160(2021).
 - [65] Y. Chen, Y. Liu, R. Lu, Y. Mizuno, J. Shu, X. Xue, Q. Yuan, Y. Zhao, *Stringent axion constraints with Event Horizon Telescope polarimetric measurements of M87*, Nature Astron. **6**(5), 592 (2022).
 - [66] K. Nomura, K. Saito, J. Soda, *Observing axions through photon ring dimming of black holes*, Phys. Rev. D **107**, 123505 (2023).
 - [67] S. Shakeri, F. Hajkarim, *Probing Axions via Light Circular Polarization and Event Horizon Telescope*, J. Cosmol. Astropart. Phys. **04**, 017 (2023).
 - [68] R. Yao, X. Bi, J. Wang, P. Yin, *Probing Axions via Light Circular Polarization and Event Horizon Telescope*, Phys. Rev. D **107**, 043031 (2023).
 - [69] A. D. Plascencia and A. Urbano, *Black hole superradiance and polarization-dependent bending of light*, J. Cosmol. Astropart. Phys. **04** 059 (2018).
 - [70] I. T. Drummond, S. J. Hathrell, *QED vacuum polarization in a background gravitational field and its effect on the velocity of photons*, Phys. Rev. D **22**, 343 (1980).
 - [71] R. D. Daniels and G. M. Shore, *“Faster than light” photons and rotating black holes*, Phys. Lett. B **367**, 75 (1996).
 - [72] R. G. Cai, *Propagation of vacuum polarized photons in topological black hole spacetimes*, Nucl. Phys. B **524**, 639 (1998).
 - [73] H. T. Cho, *“Faster than light” photons in dilaton black hole spacetimes*, Phys. Rev. D **56**, 6416 (1997).
 - [74] V. A. De Lorenci, R. Klippert, M. Novello, J. M. Salim, *Light propagation in nonlinear electrodynamics*, Phys. Lett. B **482**, 134 (2000).
 - [75] N. Breton, *Geodesic structure of the Born-Infeld black hole*, Class. Quantum Grav. **19**, 601 (2002).
 - [76] J. O. Shipley, and S. R. Dolan, *Binary black hole shadows, chaotic scattering and the Cantor set*, Class. Quantum Grav. **33**, 175001 (2016).
 - [77] A. Bohn, W. Thrope, F. Hbert, K. Henriksson, and D. Bunandar, *What does a binary black hole merger look like?*, Class. Quantum Grav. **32**, 065002 (2015), [arXiv: 1410.7775].
 - [78] M. Wang, S. Chen, J. Jing, *Shadows of Bonnor black dihole by chaotic lensing*, Phys. Rev. D **97**, 064029 (2018).
 - [79] T. Johannsen, *Photon Rings around Kerr and Kerr-like Black Holes*, Astrophys. J. **777**, 170 (2013).
 - [80] R. Roy, U. Yajnik, *Evolution of black hole shadow in the presence of ultralight bosons*, Phys. Lett. B **803**, 135284 (2020).
 - [81] Z. Younsi, A. Zhidenko, L. Rezzolla, R. Konoplya and Y. Mizuno, *New method for shadow calculations: Application to parametrized axisymmetric black holes*, Phys. Rev. D **94**, 084025 (2016).
 - [82] M. Wang, S. Chen and J. Jing, *Chaotic shadow of a non-Kerr rotating compact object with quadrupole mass*, Phys. Rev. D **98** 104040 (2018).
 - [83] F. Long, S. Chen, M. Wang, J. Jing, *Shadow of a disformal Kerr black hole in quadratic degenerate higher-order scalar-tensor theories*, Eur. Phys. J. C **80**, 1180 (2020).
 - [84] A. Payez, C. Evoli, T. Fischer, M. Giannotti, A. Mirizzi and A. Ringwald, *Revisiting the SN1987A gamma-ray limit on ultralight axion-like particles*, J. Cosmol. Astropart. Phys. **1502**, 006 (2015).
 - [85] MAGIC Collaboration, *Constraints on axion-like particles with the Perseus Galaxy Cluster with MAGIC*, Phys. Dark Univ. **44**, 101425 (2024), arXiv:2401.07798
 - [86] D. Schwarz, J. Goswami, A. Basu, *Geometric optics in the presence of axionlike particles in curved spacetime*, Phys. Rev. D **103**, L081306 (2021), arXiv: 2003.10205.